



HAL
open science

A SEMI-PARAMETRIC ESTIMATION FOR MAX-MIXTURE SPATIAL PROCESS

M Ahmed, V Maume-Deschamps, P. Ribereau, C. Vial

► **To cite this version:**

M Ahmed, V Maume-Deschamps, P. Ribereau, C. Vial. A SEMI-PARAMETRIC ESTIMATION FOR
MAX-MIXTURE SPATIAL PROCESS. 2017. hal-01617358v1

HAL Id: hal-01617358

<https://hal.science/hal-01617358v1>

Preprint submitted on 16 Oct 2017 (v1), last revised 4 Dec 2017 (v2)

HAL is a multi-disciplinary open access archive for the deposit and dissemination of scientific research documents, whether they are published or not. The documents may come from teaching and research institutions in France or abroad, or from public or private research centers.

L'archive ouverte pluridisciplinaire **HAL**, est destinée au dépôt et à la diffusion de documents scientifiques de niveau recherche, publiés ou non, émanant des établissements d'enseignement et de recherche français ou étrangers, des laboratoires publics ou privés.

A SEMI-PARAMETRIC ESTIMATION FOR MAX-MIXTURE SPATIAL PROCESS

M. AHMED, V. MAUME-DESCHAMPS, P. RIBEREAU, AND C. VIAL

ABSTRACT. We proposed a semi-parametric estimation procedure in order to estimate the parameters of a max-mixture model and also of a max-stable model (inverse max-stable model) as an alternative to composite likelihood. A good estimation by the proposed estimator required the dependence measure to detect all dependence structures in the model, especially when dealing with the max-mixture model. We overcame this challenge by using the *F-madogram*. The semi-parametric estimation was then based on a quasi least square method, by minimizing the square difference between the theoretical F-madogram and an empirical one. We evaluated the performance of this estimator through a simulation study. It was shown that on an average, the estimation is performed well, although in some cases, it encountered some difficulties. We apply our estimation procedure to model the daily rainfalls over the East Australia.

1. INTRODUCTION

In climate changes, one of the main characteristic of the event is its spatial dependence. The dependencies may be strong even for large distances as the heat waves or they may be strong at short distances and weak at larger distances, as the sevenol events. In these events many dependence structures may arise, for example, asymptotic dependence, asymptotic independence, or both [36]. These dependence structures could be (receptively) max-stable, inverse max-stable and max-mixture spatial processes.

The estimation of the parameters of these processes remains a difficulty. The usual way to estimate parameters in spatial contexts is to maximize the composite likelihood. For example, in [27], [14] and many others, the composite likelihood maximization is used to estimate the parameters of max-stable processes. In [5] and [36], it is used to estimate the parameters of max-mixture processes. Nevertheless, the estimation does not perform well in some cases; moreover, it seems to have difficulties estimating the inverted max-stable part.

For the motivation above, we propose a semi-parametric estimation procedure as an alternative to composite likelihood maximization for max-mixture and also for max-stable (resp. inverse max-stable) processes. Our procedure is a least square method on the *F-madogram*; that is, we minimize the difference between the theoretical *F-madogram* and the empirical one. Some

Key words and phrases. Spatial dependence measures, asymptotic dependence/independence, max-stable process, max-mixture, madogramme.

of literature deals with semi-parametric estimation in modeling spatial extremes. For example, [26] and [1] provided semi-parametric estimators of extremal indexes. In [8], another semi-parametric procedure to estimate model parameters is introduced. It is based on fitting the theoretical extremogram with the empirical one by non-linear least square for the isotropic space-time Brown-Resnick max-stable process. The semi-parametric procedure proposed in this study is based on this article.

In semi-parametric procedure (LS-madogram), we begin by recalling the definition of the F -madogram and calculate it for max-mixture spatial processes. Then, we prove that LS-madogram leads to consistent estimation of the parameters, provided that they are identified by the F -madogram. A simulation study is conducted in order to evaluate the estimation performance and to compare LS-madogram estimation with the maximization of the composite likelihood. It shows, in general, that the estimation performs well, although it encounters some difficulties, which are discussed.

Section 2 is dedicated to the main tools which used in this study; it contains some of spatial dependence measures and also three different extreme spatial processes with different dependence structures (asymptotic dependence/independence and a mixture of them) are presented in this section. In Section 3, we calculate an expression for the F -madogram of max-mixture models. Section 4 is devoted to two estimation procedures of the parameters of max-mixture processes; Composite likelihood and LS-madogram. A simulation study is conducted, which allows us to evaluate the performance of the estimation procedure (Section 5). Section 6 is devoted in modelling rainfall real data in East Australia. Finally, concluding remarks are discussed in Section 7.

2. MAIN TOOLS USED IN THE STUDY

Throughout this study, the spatial process $X := \{X(s), s \in \mathbb{S}\}$, $\mathbb{S} \in \mathbb{R}^d$ is assumed to be strongly stationary and isotopic.

2.1. Dependence measures. Important properties of a spatial process are described by its spatial dependence structure and lots of measures are defined in the literature to better understand the dependence in real spatial data.

At first, the **upper tail dependence coefficient** χ measures the association degree between the processes at two locations and becomes a function depending on the distance between the two sites; see [6, 30]. It is defined for a stationary spatial process X on $\mathbb{S} \subset \mathbb{R}^2$ with margin F

$$(2.1) \quad \chi(h) = \lim_{u \rightarrow 1^-} \mathbb{P}(F(X(s+h)) > u | F(X(s)) > u).$$

The process is said AI (resp. AD) if for all $h \in \mathbb{S}$ $\chi(h) = 0$ (resp. $\chi(h) \neq 0$).

For any h the coefficient $\chi(h)$ can alternatively be expressed as the limit when $u \rightarrow 1^-$ of the function defined on $\mathbb{S} \times [0, 1]$ into $[0, 1]$, by

$$(2.2) \quad \chi(h, u) = 2 - \frac{\log \mathbb{P}(F(X(s)) < u, F(X(t)) < u)}{\log \mathbb{P}(F(X(s)) < u)}, \text{ for } h \in \mathbb{S}, u \in [0, 1].$$

Such that, $\chi(h) = \lim_{u \rightarrow -1} \chi(h, u)$.

For asymptotic independent processes, the behaviour of the conditional probability with respect to u suggests that the asymptotic independence could not be detected as it appears for u very near to 1. Thus, it suggests that the function χ is more useful to study asymptotic dependence than asymptotic independence. This is why the authors in [11], introduced an alternative dependence coefficient called **lower tail dependence coefficient** $\bar{\chi}$. This quantity measures the strength of asymptotic independence of a process. The function $\bar{\chi}$ defined from \mathbb{S} into $] - 1, 1[$ and for any $(s, s + h) \in \mathbb{S}^2$

$$(2.3) \quad \bar{\chi}(h, u) = \frac{2 \log \mathbb{P}(F(X(s)) > u)}{\log \mathbb{P}(F(X(s)) > u, F(X(s + h)) > u)} - 1, \quad 0 \leq u \leq 1$$

such that, $\bar{\chi}(h) = \lim_{u \rightarrow 1} \bar{\chi}(h, u)$.

If $\bar{\chi}(h) = 1$ for all h , the spatial process is asymptotically dependent. Otherwise, the process is said to be asymptotically independent. Furthermore, if $\bar{\chi} \in]0, 1[$ (resp. $] - 1, 0[$) the two locations s and $s + h$ (for any s) are asymptotically positively associated (resp. asymptotically negatively associated).

Another important measure of dependence was introduced by [9, 29] is the extremal coefficient between two locations s and $s + h$ for any $s \in \mathbb{S}$ and $s + h \in \mathbb{S}$, and for any $x \in \mathbb{R}$ defined by

$$\theta_F(h, x) = \frac{\log(P(X(s) < x, X(s + h) < x))}{\log(P(X(s) < x))}.$$

This parameter is related to the upper tail dependence parameter; indeed if $\lim_{x \rightarrow x_F} \theta_F(h, x) = \theta(h)$ exists, we have the following relation [6].

$$\chi(h) = 2 - \theta_F(h),$$

where $x_F = \sup\{x | F(x) < 1\}$. Then, $P(X(s) < x, X(s + h) < x)$ may be approximated by $F(x)^{\theta_F(h)}$ for x large.

This coefficient is particularly useful when dealing with asymptotic dependence, but useless in case of asymptotic independence. To overcome this problem, [23] proposed a model allowing to gather all the different cases of dependence depending on the value of a parameter in another words, smoothly linking asymptotic dependence and independence. Such that, for X with unit Fréchet margin and for all $(s, s + h) \in \mathbb{S}^2$ the pairwise survivor function

$$(2.4) \quad \mathbb{P}(X(s) > x, X(s + h) > x) = \mathcal{L}_h(x) x^{-1/\eta(h)}, \quad \text{as } x \rightarrow \infty$$

satisfy. Where \mathcal{L}_h is a slowly varying function and $\eta(h) \in (0, 1]$ is the **tail dependence coefficient**. This coefficient determines the decay rate of the bivariate tail probability for large x . The interest of this simple modelisation, which appears to be quite general, is that the coefficient $\eta(h)$ provides

a measure of the extremal dependence of $X(s)$ and $X(x+h)$. Such that, $\mathcal{L}(x) \not\rightarrow 0$ (resp. $0 < \eta(h) < 1$ and $\mathcal{L}(x) \not\rightarrow 0$), corresponds to asymptotic dependence (resp. asymptotic independence); see [6, 23]. Finally, it is important to see the relations between η and $\bar{\chi}$. If equation (2.4) is satisfied, then $\bar{\chi}(h) \rightarrow 2\eta(h) - 1$.

Another classical tool often used in geostatistics is the variogram. But for spatial processes with Fréchet, the quantity of dependence strength will not exist in variogram, because the marginal laws, and thus, have no order 2 moments. We shall use the *F-madogram* introduced in [12] which is defined for any spatial process X with univariate margin F and for all $(s, t) \in \mathbb{S}^2$

$$(2.5) \quad \nu^F(s-t) = \frac{1}{2} \mathbb{E}|F(X(s)) - F(X(t))|.$$

2.2. Spatial extreme models.

2.3. Max-stable model. Max-stable processes are the extension of the multivariate extreme value theory to the infinite dimensional setting [8]. Let $T := (T(s), s \in \mathbb{S})$ be a stochastic process. If there exist two sequences of continuous functions $(a_n(\cdot) > 0, n \in \mathbb{N})$ and $(b_n(\cdot) \in \mathbb{R}, n \in \mathbb{N})$ such that for all $n \in \mathbb{N}$ and n i.i.d. X_1, \dots, X_n and X a process, such that

$$(2.6) \quad \max_{i=1, \dots, n} \frac{X_i - b_n}{a_n} \xrightarrow{d} X, \quad n \rightarrow \infty,$$

then $X := \{X(s), s \in \mathbb{S}\}$ is a max-stable process [17]. When for all $n \in \mathbb{N}$, $a_n = 1$ and $b_n = 0$, the margin distribution of the process X is unit Fréchet, that is for any $s \in \mathbb{S}$ and $x > 0$,

$$F(x) := P(X(s) \leq x) = \exp[-1/x].$$

[16] proved that a max-stable process X can be constructed by using a random process and a Poisson process. This representation is named the **spectral representation**. Let X be a max-stable process on \mathbb{S} . Then there exists $\{\xi_i, i \geq 1\}$ i.i.d Poisson point process on $(0, \infty)$, with intensity $d\xi/\xi^2$ and a sequence $\{W_i, i \geq 1\}$ of i.i.d. copies of a positive process $W = (W(s), s \in \mathbb{S})$, such that $\mathbb{E}[W(s)] = 1$ for all $s \in \mathbb{S}$ such that

$$(2.7) \quad X =^d \max_{i \geq 1} \xi_i W_i.$$

and

$$(2.8) \quad \mathbb{P}(X(s_1) \leq x_1, \dots, X(s_k) \leq x_k) = \exp\{-V(x_1, \dots, x_k)\},$$

where the function

$$(2.9) \quad V(x_1, \dots, x_k) = \mathbb{E} \left[\max_{\ell=1, \dots, k} \left(\frac{W(s_\ell)}{x_\ell} \right) \right].$$

is homogenous of order -1 and is named *the exponent measure*. One of the interests of the exponent measure is its interpretation in terms of dependence. In fact, the homogeneity of the exponent measure V implies

$$(2.10) \quad \max\{1/x_1, \dots, 1/x_k\} \leq V(x_1, \dots, x_k) \leq \{1/x_1 + \dots + 1/x_k\}.$$

See [7], section 8.2.2. In the inequalities (2.10), the lower (resp. upper) bound corresponds to complete dependence (resp. independence).

For simple max-stable process, **the extremal coefficient function** Θ , for any pairs of sites $(s, s+h) \in \mathbb{S}^2$ is the function Θ defined on \mathbb{S} (or in \mathbb{R}^+ in isotropic case) with values in $[1, 2]$ by

$$(2.11) \quad \mathbb{P}(X(s) \leq x, X(s+h) \leq x) = \exp\{-\Theta(h)/x\}, \quad x > 0$$

where,

$$(2.12) \quad \Theta(h) = \mathbb{E}[\max\{W(s), W(s+h)\}] = V(1, 1) \in [1, 2].$$

If for any $h \in \mathbb{S}$, $\Theta(h) = 1$ (resp. $\Theta(h) = 2$), then we have complete dependence (resp. complete independence). The case $1 < \Theta(h) < 2$, for all $h \in \mathbb{S}$ corresponds to asymptotic dependence. Remark that, in simple max-stable process, the coefficients Θ and θ_F coincide.

Furthermore, it is easy to see the relationship between Θ and χ ; see [36] for any $h \in \mathbb{S}$

$$(2.13) \quad \Theta(h) = 2 - \chi(h).$$

In the max-stable case, [12] gives the relation for all $h \in \mathbb{S}$,

$$(2.14) \quad \Theta(h) = \frac{1 + 2\nu^F(h)}{1 - 2\nu^F(h)},$$

which appears to be helpful to estimate the extremal coefficient Θ . The max-stable process X with pairwise distribution function is given by the following equation, for all $(s, s+h) \in \mathbb{S}^2$,

$$(2.15) \quad \mathbb{P}(X(s) \leq x_1, X(s+h) \leq x_2) = \exp\{-V_h(x_1, x_2)\},$$

In this study, we provide three examples of well-known max-stable models represented by different exponent measures V .

Smith Model (Gaussian extreme value model) [31] with unit Fréchet margin and exponent measure

$$(2.16) \quad V_h(x_1, x_2) = \frac{1}{x_1} \Phi\left(\frac{\tau(h)}{2} + \frac{1}{\tau(h)} \log \frac{x_2}{x_1}\right) + \frac{1}{x_2} \Phi\left(\frac{\tau(h)}{2} + \frac{1}{\tau(h)} \log \frac{x_1}{x_2}\right);$$

$\tau(h) = \sqrt{h^T \Sigma^{-1} h}$ and $\Phi(\cdot)$ the standard normal cumulative distribution function. For isotropic case $\tau(h) = \sqrt{\frac{1}{\sigma} \|h\|^2}$.

The pairwise extremal coefficient equals

$$(2.17) \quad \Theta(h) = 2\Phi\left(\frac{\tau(h)}{2}\right).$$

Brown-Resnik Model [22] with unit Fréchet margin and exponent measure

$$(2.18) \quad V_h(x_1, x_2) = \frac{1}{x_1} \Phi\left(\frac{\sqrt{2\gamma(h)}}{2} + \frac{1}{\sqrt{2\gamma(h)}} \log \frac{x_2}{x_1}\right) + \frac{1}{x_2} \Phi\left(\frac{\sqrt{2\gamma(h)}}{2} + \frac{1}{\sqrt{2\gamma(h)}} \log \frac{x_1}{x_2}\right);$$

$2\gamma(h)$ is a variogram and $\Phi(\cdot)$ the standard normal cumulative distribution function. The pairwise extremal coefficient given by

$$(2.19) \quad \Theta(h) = 2\Phi\left(\frac{\sqrt{2\gamma(h)}}{2}\right).$$

Truncated extremal Gaussian Model (TEG) [28] with unit Fréchet margin and exponent measure

$$(2.20) \quad V_h(x_1, x_2) = \left(\frac{1}{x_1} + \frac{1}{x_2}\right) \left[1 - \frac{\alpha(h)}{2} \left(1 - \sqrt{1 - 2(\rho(h) + 1) \frac{x_1 x_2}{(x_1 + x_2)^2}}\right)\right].$$

The extremal coefficient is given by

$$(2.21) \quad \Theta(h) = 2 - \alpha(h) \left\{1 - \left(\frac{1 - \rho(h)}{2}\right)^{1/2}\right\}$$

where $\alpha(h) = \mathbb{E}\{|\mathcal{B} \cap (h + \mathcal{B})|\} / \mathbb{E}[|\mathcal{B}|]$,

where \mathcal{B} is a random set which can consider it a disk with fixed radius r . in order to $\alpha(h) = \{1 - h/2r\}_+$; See [15]. In such a case, $\chi(h) = 0, \forall h \geq 2r$.

2.4. Inverse Max-stable processes. If we choose a threshold too low, we may miss the dependence structure. In other words, in theoretical study, the limiting distribution of extremes tends to be independent but in practice, this limit could never be achieved (see [15, 32]).

[36] proposed a class of asymptotically independent processes obtained by inverting max-stable processes. These processes are called **inverse max-stable processes**; they satisfy the survivor function (2.4). Let $X' := \{X'(s), s \in \mathbb{S}\}$ be a max-stable process with unit Fréchet margin, such that for all $s \in \mathbb{S} \subset \mathbb{R}^2$

$$(2.22) \quad X'(s) = \mu^{-1} \max_{i \geq 1} W_i^+(s) / \xi_i, \quad s \in \mathbb{S}$$

where ξ_i is a Poisson point process on $(0, \infty)$ with intensity $d\xi$ and $W_i(s)$ are i.i.d. copies of a continuous process W independent of $\{\xi_i\}$. Let $g : (0, \infty) \mapsto (0, \infty)$ be defined by $g(x) = -1/\log\{1 - e^{-1/x}\}$. Set $X(s) = g(X'(s))$. Then, $X := \{X(s), s \in \mathbb{S}\}$ is an asymptotic independent spatial process with unit Fréchet margin. The d-dimensional joint survivor function is

$$(2.23) \quad \mathbb{P}(X(s_1) > x_1, \dots, X(s_d) > x_d) = \exp\{-V(g(x_1), \dots, g(x_d))\}$$

where V is the exponent measure of the process X' defined in equation (2.9). The tail dependent coefficient is given by $\eta(h) = 1/\Theta(h)$, where $\Theta(h)$ is the extremal coefficient of the max-stable process X' . Moreover, we have $\tilde{\chi}(h) = 2/\Theta(h) - 1$.

2.5. Max-mixture model. In spatial contexts, specifically in an environmental domain, many scenarios of dependence could arise and AD and AI might cohabite. The work by [36] provides a flexible model called max-mixture.

Let $X := \{X(s), s \in \mathbb{S}\}$ be a max-stable process with extremal coefficient

$\Theta(h)$ and bivariate distribution function F_X , and let $Y := \{Y(s), s \in \mathbb{S}\}$ be an asymptotically independent spatial process whose coefficient tail dependence $\eta(h)$ is well defined, has the bivariate distribution function F_Y and satisfies the asymptotic relation (2.4). Assume that X and Y are independent, and that each of them has Fréchet margin. Let $a \in [0, 1]$ and

$$(2.24) \quad Z(s) = \max\{aX(s), (1-a)Y(s)\}, \quad s \in \mathbb{S},$$

then Z is a max-mixture process has unit Fréchet marginals and pairwise survivor function

$$(2.25) \quad \mathbb{P}(Z(s) > z, Z(t) > z) \sim \frac{a\{2 - \Theta(h)\}}{z} + \frac{(1-a)^{1/\eta(h)}}{z^{1/\eta(h)}} + O(z^{-2}), \quad z \rightarrow \infty.$$

Assume there exists finite $h^* = \inf\{h : \Theta(h) \neq 0\}$; then,

$$(2.26) \quad \chi(h) = a(2 - \Theta(h))$$

and

$$(2.27) \quad \bar{\chi}(h) = \mathbb{1}_{[h^* < h]}(h) + (2\eta(h) - 1)\mathbb{1}_{[h^* \geq h]}.$$

Rk. If there exists finite $h^* = \inf\{h : \Theta(h) \neq 0\}$, then Z is asymptotically dependent up to distance h^* and asymptotically independent for larger distances. Only asymptotic dependence or asymptotical independence in Z is achieved by the bounds $a = 0$ and $a = 1$, respectively.

[5] used this kind of models to allow asymptotical dependence and independence to be present at a short and intermediate distance respectively; furthermore, the process is independent at a long distance. This structure has been made by combining the truncated Gaussian extremal max-stable process with an asymptotically independent process.

3. F -MADOGRAM FOR MAX-MIXTURE SPATIAL PROCESS

In extreme value theory and therefore for spatial extremes, one of the main concerns is to find a dependence measure that can quantify the dependences between locations. The χ and $\bar{\chi}$ dependence measures are designed to quantify asymptotic dependence and asymptotic independence respectively. Max-mixture processes have been introduced in order to provide both behaviors. We are then faced with the question of finding an adapted tool which would give information on more than one dependence structure; See equations (2.26) and (2.27).

In [12], the F -madogram has been introduced for max-stable processes. There exists several definitions of madograms. For example, in [25], the λ -madogram is considered in order to take into account the dependence information from the exponent measure $V_h(u, v)$ when $u \neq v$. This λ -madogram has been extended in [19] to evaluate the dependence between two observations located in two disjoint regions in \mathbb{R}^2 . [20] adopted an F -madogram suitable for asymptotic independence instead of asymptotic dependence only. Finally, [3] used F -madogram as a test statistic for asymptotic independence bivariate maxima.

Below, we calculate $\nu^F(h)$ for a max-mixture process. It appears that contrary to χ and $\bar{\chi}$, it combines the parameters coming from the AD and the AI parts.

Proposition 1. *Let Z be a max-mixture process, with mixing coefficient $a \in [0, 1]$. Let X be its max-stable part with extremal coefficient $\Theta(h)$. Let Y be its inverse max-stable part with tail dependence coefficient $\eta(h)$. Then, the F -madogram of Z is*

$$(3.1) \quad \nu^F(h) = \frac{a(\Theta(h) - 1)}{a(\Theta(h) - 1) + 2} - \frac{a\Theta(h) - 1}{2a\Theta(h) + 2} - \frac{1/\eta(h)}{a\Theta(h) + (1-a)/\eta(h) + 1} \beta\left(\frac{a\Theta(h) + 1}{(1-a)}, 1/\eta(h)\right),$$

where β is beta function.

Proof. We have

$$(3.2) \quad \nu^F(h) = \frac{1}{2} \mathbb{E}|F(Z(s)) - F(Z(s+h))|.$$

The equality $|a - b|/2 = \max(a, b) - (a + b)/2$ leads to

$$(3.3) \quad \nu^F(h) = \mathbb{E}[\max(F(Z(s)), F(Z(s+h)))] - \mathbb{E}[F(Z(s))].$$

Let $M(h) = \max(F(Z(s)), F(Z(s+h)))$, we have:

$$(3.4) \quad \mathbb{P}(M(h) \leq u) = \mathbb{P}(Z(s) \leq F^{-1}(u), Z(s+h) \leq F^{-1}(u)).$$

From assumptions of the max-mixture spatial process Z , the corresponding probability distribution function is

$$(3.5) \quad \mathbb{P}(Z(s) \leq z_1, Z(s+h) \leq z_2) = e^{-aV_X^h(z_1, z_2)} \left[e^{\frac{-(1-a)}{z_1}} + e^{\frac{-(1-a)}{z_2}} - 1 + e^{-V_Y^h(g(z_1), g(z_2))} \right],$$

where V_X (resp. V_Y) corresponding to the exponent measures of X (resp. Y) and $g(z) = -1/\log(1 - e^{\frac{-(1-a)}{z}})$. That leads to

$$\mathbb{P}(M(h) \leq u) = u^{a\Theta(h)} [2u^{(1-a)} - 1 + (1 - u^{(1-a)})^{1/\eta(h)}], \quad u \in [0, 1].$$

We deduce that

$$(3.6) \quad \mathbb{E}[M(h)] = \int_0^1 u f_M(h)(u) du = \frac{2a(\Theta(h) - 1) + 2}{a(\Theta(h) - 1) + 2} - \frac{a\Theta(h)}{a\Theta(h) + 1} - \frac{\beta\left(\frac{a\Theta(h) + 1}{(1-a)}, 1/\eta(h)\right)}{\eta(h)(1-a) \left[\frac{a\Theta(h) + 1}{(1-a)} + (1/\eta(h)) \right]}.$$

where $f_M(h)$ is the density of $M(h)$. Recall that $\mathbb{E}(F(Z(s))) = \frac{1}{2}$ because $F(Z(s)) \sim \mathcal{U}([0, 1])$ and return to equation (3.3) to get equation (3.1). \square

It is easy to deduce from the PQD (positive quadrant dependence) of Z that $\nu^F(h) = 0$ (resp. $\nu^F(h) = 1/6$) when $Z(s)$ and $Z(s+h)$ are perfectly dependent (resp. independent). In the particular cases where $a = 1$ or $a = 0$, Proposition 1 reduces to known results for max-stable processes (see

[12]) and inverse max-stable processes (see [20]). Such that the F -madogram for a max-stable spatial process is given by

$$(3.7) \quad 2\nu^F(h) = \frac{\Theta(h) - 1}{\Theta(h) + 1}.$$

and the F -madogram of an asymptotically independent spatial process is given by

$$(3.8) \quad 2\nu^F(h) = \frac{1 - \eta(h)}{1 + \eta(h)}$$

In order to have a comprehensive view of the behavior of $\nu^F(h)$, we have plotted in Figure 1. below $h \rightsquigarrow \nu^F(h)$. We have considered two max-mixture models MM1 and MM2 described as the following: **MM1** max-mixture between a TEG max-stable process X ; and an inverse Smith max-stable process Y ; **MM2** max-mixture between X in MM1; and inverse TEG max-stable process Y .

In this Figure and for the two models MM1 and MM2, $\nu^F(h)$ has two sill one corresponding to X and the second corresponding to Y . This is completely in accordance with the nested variogram concept as presented in [35]. In data analysis, these two levels of the sill gives the researcher a hint about whether there is more than one spatial dependence structure in the data.

As consequence F -madogram expresses with all the model parameters is useful for the parameter estimation. On the contrary, when one considers the tail dependence function $\chi(h)$, it only involves the parameters from the max-stable part. The lower tail dependence function $\bar{\chi}(h)$ only involves the parameters from the inverse max-stable part.

4. MODEL INFERENCE

This section is devoted to the parametric inference for max-mixture processes. We begin with the presentation of the maximum composite likelihood estimation, then we present the least squares madogram.

4.1. Parametric Estimation using Composite Likelihood. Consider $(Z^k(s_1), \dots, Z^k(s_D))$, $k = 1, \dots, N$, be N independent copies of a spatial process $(Z(s))_{s \in \mathbb{S}}$, observed at D locations s_1, \dots, s_D . Composite likelihood inference is appropriate approach in estimating the parameter models of a spatial process X ; [24, 33]. Asmpototic properties of this estimator has been proved in [13]. This approach has been applied successfully to spatial max-stable processes by [14] and [27] and is also used to identify the parameters of data exceedances over a large threshold, for example, [4] and [32].

Our interest in this study lies in max-mixture models; two studies [5] and [36] highlight on these models; therefore, we will take the composite likelihood proposed by [5] as the control for evaluating the performance of the proposed non-linear least square estimator, which will be introduced in the next section.

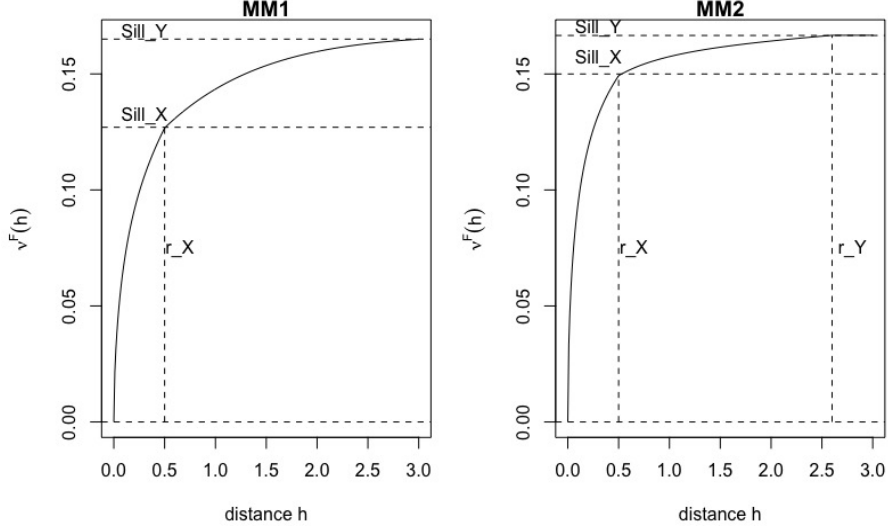


FIGURE 1. $h \rightsquigarrow \nu^F(h)$ for the max-mixture processes models MM1 and MM2. In MM1, X has correlation function $\rho(h) = \exp(-h/\theta_X)$, $r_X = 0.25$ and fixed radius $\theta_X = 0.2$ and Y has $\Sigma = \sigma_Y \mathbf{I}_d$, $\sigma_Y = 0.6$. In MM2, X as the same setting in MM1 and Y has $\rho_Y(h) = \exp(-h/\theta_Y)$, $\theta_Y = 0.8$ and fixed radius $r_Y = 1.35$. For the two models, we set $a = 0.5$.

If the pairwise density of Z can be computed and its parameter ψ is identifiable, then it is possible to estimate ψ by maximizing the pairwise weighted log likelihood. For simplicity, we denote Z_i^k for $Z^k(s_i)$. Let

$$\hat{\psi}_L = \max_{\psi} \mathcal{P}(\psi),$$

where

$$(4.1) \quad \mathcal{P}(\psi) = \sum_{k=1}^N \sum_{i=1}^{D-1} \sum_{j>i}^D w_{ij} \log \mathcal{L}(Z_i^k, Z_j^k; \psi) =: \sum_{k=1}^N \mathcal{P}_k(\psi).$$

where \mathcal{L} is the likelihood of the pair (Z_i^k, Z_j^k) and $w_{i,j} \geq 0$ is the weight that specifies the contribution for each pair. In [4], it is suggested to take $w_{i,j} = 0$ for any pair separated by distance over a specific value δ and $w_{i,j} = 1$ otherwise.

In [10], it is suggested to consider a censor approach of the likelihood, taking into account a threshold. This approach has been adopted in this study. Let $G(\cdot, \cdot)$ be a pairwise distribution function and consider the thresholds u_1 and u_2 ; the likelihood contribution is

$$\mathcal{L}(z_1, z_2; \psi) = \begin{cases} \partial_{12}^2 G(z_1, z_2; \psi) & \text{if } z_1 > u_1, z_2 > u_2, \\ G(z_1, z_2; \psi) & \text{if } z_1 \leq u_1, z_2 \leq u_2, \end{cases}$$

where ∂_i is the differentiation with respect to the variable z_i . In [36], the censored likelihood is used in order to improve the estimation of the parameters related to asymptotic independence. This censored approach was also

applied by [5] for the estimation of parameters of max-mixture processes. In this paper, the replications Z^1, \dots, Z^N of Z are assumed to be α -mixing rather than independent. We denote generically by ψ the parameters of the model. In [5], it is proved, under some smoothness assumptions on the composite likelihood, that the composite maximum likelihood estimator $\hat{\psi}_L$ for max-mixture processes is asymptotically normal as N goes to infinity with asymptotic variance

$$\mathcal{G}(\psi) = \mathcal{J}(\psi)[\mathcal{K}(\psi)]^{-1}\mathcal{J}(\psi),$$

where $\mathcal{J}(\psi) = \mathbb{E}[-\nabla^2\mathcal{P}(\psi)]$, $\mathcal{K}(\psi) = \text{var}(\nabla\mathcal{P}(\psi))$. The matrix $\mathcal{G}(\psi)$ is called the Godambe information matrix (see [5] and theorem 3.4.7 in [21]). An estimator $\hat{\mathcal{J}}$ of $\mathcal{J}(\psi)$ is obtained from the Hessian matrix computed in the optimization algorithm. The variability matrix $\mathcal{K}(\psi)$ has to be estimated too. In our context, we have independent replications of Z and N is large compared with respect to the dimension of ψ . Then, we can use the outer product of the estimation of $\hat{\psi}$. Let

$$\hat{\mathcal{K}}(\psi) = N^{-1} \sum_{k=1}^N \nabla\mathcal{P}_k(\hat{\psi})\nabla\mathcal{P}_k(\hat{\psi})'$$

or by Monte Carlo simulation with explicit formula of $\mathcal{P}_k(\psi)$ (see section 5. in [33]). In the case of samples of Z satisfying the α -mixing property, the estimation of $\mathcal{K}(\psi)$ can be done using a subsampling technique introduced by [18]; this was used in [5]. Finally, model selection can be done by using the composite likelihood information criterion [34]:

$$\text{CLIC} = -2 \left[\mathcal{P}(\hat{\psi}) - \text{tr}(\hat{\mathcal{J}}^{-1}\hat{\mathcal{K}}) \right].$$

Considering several max-stable models, the one that has the smallest CLIC will be chosen. In [32], the criterion $\text{CLIC}^* = (D-1)^{-1}\text{CLIC}$ is proposed. It is close to Akaike information criterion (AIC).

4.2. Semi-parametric estimation using NLS of F-madogram. In this section, we shall define the non-linear least square estimation procedure of the parameters set ψ corresponding to the max-mixture model Z using the F -madogram. This procedure can be considered as an alternative method to the composite likelihood method.

Consider Z^t , $t = 1, \dots, T$ as copies of an isotropic max-mixture process Z with unit Fréchet marginal laws (F denotes the distribution function of a unit Fréchet law). It may be independent copies for example, if the data is recorded yearly (see [25]) or we shall consider that $(Z^t)_{t=1, \dots, T}$ satisfies an α -mixing property ([5]). Let \mathcal{H} be a finite subset of \mathbb{S} , $J(x, y) = \frac{1}{2}|x - y|$ and $Y_{h,t} = J(F(Z^t(s)), F(Z^t(s+h)))$, $t = 1, \dots, T$ and $h \in \mathcal{H}$. Therefore, for $t = 1, \dots, T$, the vectors $(Y_{h,t})_{h \in \mathcal{H}}$ have the same law and are considered either independent or α -mixing (in t). The main motivation for using the F -madogram in estimation is that it contains the dependence structure information for a fixed h of $Y_{h,t}$ (see section 3.2 in [3]).

In what follows, we make the assumption that the vectors $(Y_{h,t})_{h \in \mathcal{H}}$ are i.i.d. Note that from the definition of the F -madogram, we have $\mathbb{E}[Y_{t,h}] = \nu^F(h, \psi)$

where $\nu^F(h, \psi)$ is the F -madogram of Z with parameters ψ defined in (3.1). If Z has an unknown true parameter ψ_0 on a compact set $\Psi \subset \mathbb{R}^d$, we rewrite

$$(4.2) \quad Y_{h,t} = \nu^F(h, \psi_0) + \varepsilon_{h,t}.$$

The vectors $(\varepsilon_{h,t})_{h \in \mathcal{H}}$ are i.i.d errors with $\mathbb{E}[\varepsilon_{h,t}] = 0$ and $\text{Var}(\varepsilon_{h,t}) = \sigma_h^2 > 0$ is finite and unknown.

Let

$$(4.3) \quad \mathcal{L}(\psi) = \sum_{h \in \mathcal{H}} \frac{1}{T} \sum_{t=1, \dots, T} (Y_{t,h} - \nu^F(h, \psi))^2$$

Any vector $\hat{\psi}_T$ in Ψ which minimizes $\mathcal{L}(\psi)$ will be called a least square estimate of ψ_0 .

$$(4.4) \quad \hat{\psi}_T \in \underset{\psi \in \Psi}{\text{argmin}} \mathcal{L}(\psi).$$

Theorem 2. *Assume that $\Psi \subset \mathbb{R}^d$ is compact and that $\psi \mapsto \nu^F(h, \psi)$ is continuous for all $h \in \mathcal{H}$. We assume that the vectors $(Y_{h,t})_{h \in \mathcal{H}}$ are i.i.d. Let $(\hat{\psi}_T)_{T \in \mathbb{N}}$ be least square estimators of ψ_0 ; then, any limit point (as T goes to infinity) ψ of $(\hat{\psi}_T)_{T \in \mathbb{N}}$ satisfies $\nu(h, \psi) = \nu(h, \psi_0)$ for all $h \in \mathcal{H}$.*

remark 1. *Of course, if $\psi \rightsquigarrow (\nu(h, \psi))_{h \in \mathcal{H}}$ is injective, then theorem 2 implies that the least square estimation is consistent, i.e. $\psi_T \rightarrow \psi_0$ a.s. as T goes to infinity. In the examples considered below, it seems that the injectivity is satisfied provided $|\mathcal{H}| \geq d$, but we were unable to prove it.*

Proof. We follow the proof of Theorem II.5.1 in [2]. From (4.2), we have, for all $\psi \in \Psi$

$$\begin{aligned} \mathcal{L}(\psi) &= \sum_{h \in \mathcal{H}} \frac{1}{T} \sum_{t=1, \dots, T} (\nu^F(h, \psi_0) + \varepsilon_{h,t} - \nu^F(h, \psi))^2 \\ &= \sum_{h \in \mathcal{H}} (\nu^F(h, \psi_0) - \nu^F(h, \psi))^2 \\ &\quad + \frac{2}{T} \sum_{h \in \mathcal{H}} (\nu^F(h, \psi_0) - \nu^F(h, \psi)) \left(\sum_{t=1, \dots, T} \varepsilon_{h,t} \right) + \sum_{h \in \mathcal{H}} \frac{1}{T} \sum_{t=1, \dots, T} \varepsilon_{h,t}^2. \end{aligned}$$

From the law of large numbers, we have

$$\frac{1}{T} \sum_{h \in \mathcal{H}} \sum_{t=1, \dots, T} \varepsilon_{h,t}^2 \rightarrow \sum_{h \in \mathcal{H}} \sigma_h^2 \quad \text{a.s. as } T \rightarrow \infty$$

and for any $h \in \mathcal{H}$,

$$\frac{1}{T} \sum_{t=1, \dots, T} \varepsilon_{h,t} \rightarrow 0 \quad \text{a.s.}$$

Therefore,

$$\mathcal{L}(\psi) \rightarrow \sum_{h \in \mathcal{H}} \sigma_h^2 + \sum_{h \in \mathcal{H}} (\nu^F(h, \psi_0) - \nu^F(h, \psi))^2 \quad \text{a.s. as } T \rightarrow \infty.$$

Take a sequence $(\hat{\psi}_T)_{T \in \mathbb{N}}$ of least square estimators, taking if necessary a subsequence, we may assume that it converges to some $\psi^* \in \Psi$. Using the continuity of $\psi \rightsquigarrow \nu^F(h, \psi)$, we have

$$\mathcal{L}(\hat{\psi}_T) \rightarrow \sum_{h \in \mathcal{H}} \sigma_h^2 + \sum_{h \in \mathcal{H}} (\nu^F(h, \psi_0) - \nu^F(h, \psi^*))^2 \quad \text{a.s. as } T \rightarrow \infty.$$

Since $\hat{\psi}_T$ is a least square estimator, $\mathcal{L}(\hat{\psi}_T) \leq \mathcal{L}(\psi_0) \rightarrow \sum_{h \in \mathcal{H}} \sigma_h^2$. It follows

that

$$\sum_{h \in \mathcal{H}} (\nu^F(h, \psi_0) - \nu^F(h, \psi^*))^2 = 0$$

and thus $\nu(h, \psi^*) = \nu(h, \psi_0)$ for all $h \in \mathcal{H}$. \square

The asymptotic normality of the least square estimators should also be obtained by following, e.g., [8] and using the asymptotic normality of the F -madogram obtained in [12]. Nevertheless, the calculation of the asymptotic variance will require to calculate the covariances between $\nu^F(h_1, \psi)$ and $\nu^F(h_2, \psi)$, which is not straightforward.

5. SIMULATION STUDY

This section is devoted to some simulations in order to evaluate the performance of the least square estimator and to compare it with the maximum composite likelihood estimator. Recall that $\hat{\psi}_T$ denotes the least square estimator of the parameter vector ψ and $\hat{\psi}_L$ denotes the composite likelihood estimator.

5.1. Outline the estimation experiment. In order to evaluate the performance of the non-linear least square estimator $\hat{\psi}_T$ as defined in (3.1), we have generated data from the model MM1 above with the same setting. The estimator $\hat{\psi}_T$ has been compared with true one ψ_0 and also with parameters estimated by composite likelihood estimator $\hat{\psi}_L$ proposed in [5] for the same data. We considered 50 sites randomly and uniformly distributed in the square $\mathcal{A} = [0, 1]^2$ with the same setting .

We have generated $T = 1000$ i.i.d observations for each site. These experiments replicated $J = 100$ time. We have considered several mixing parameters: $a := \{0, 0.25, 0.5, 0.75, 1\}$. For the composite likelihood estimator $\hat{\psi}_L$, we used the censored procedure with the threshold $u = 0.9$ of empirical quantile of data at each site. The fitting of $\hat{\psi}_L$ was done using the code which was used in [5] with some modifications.

5.2. Results on the parameters estimate. The following boxplots represent the error of estimated parameters, that is $(\hat{\psi}_T - \psi_0)$ and $(\hat{\psi}_L - \psi_0)$. Figure 2. display the performance of estimators for model MM1. Generally, the estimators above worked well, although the variability in some estimates were relatively large, especially for the asymptotic independence parameters. It also shows some bias in the estimation of asymptotic independence model parameters.

It is well known that asymptotic independence is difficult to estimate, because the dependence between the process locations may decay very slowly when the distance increases (see [15]). Therefore, the estimation accuracy of the parameters is very sensitive, especially when dealing with more than one dependence structures. On one other hand, the fitting of $\alpha(h)$ which appears in TEG models in (2.20), is delicate and might quite get different estimates efficiency results with different data [14]. Furthermore, the dependence measures does not have all dependence information [12].

To compare the estimation efficiency between the estimators $\hat{\psi}_T$ and $\hat{\psi}_L$, the root mean square error (RMSE) was calculated for each estimated parameter based on the $J = 100$ experiments [37, 38]: $\hat{\psi}_j$ denotes the estimation (either least square or composite likelihood estimation) on the j th experiment.

$$(5.1) \quad \text{RMSE} = \left[J^{-1} \sum_{j=1}^J (\hat{\psi}_j - \psi)^2 \right]^{1/2},$$

The barplot in Figure 3 display the RMSE for each parameter of MM1 model. We see on these barplots that when a is close to 0 ($a = 0; 0.25$), the estimator $\hat{\psi}_T$ over-performs the estimator $\hat{\psi}_L$ and vice versa when $a \in \{0.75, 1\}$. For $a = 0.5$ the performance of the two estimators seems relatively equivalent.

5.3. Asymptotic normality. Since finding the asymptotic normality of the estimator ψ_T is difficult, we will test it by a simulation. From the large-sample convergence properties of the estimators, we can see if the distribution of the errors between the arbitrarily estimates $\hat{\psi}_T$ and the true one ψ_0 close to normal distribution. In Figure 4, the graphs represent the distributions of the errors of each estimate parameters of MM1 model for $a := \{0, 0.25, 0.75, 1\}$. We adopted the same $J = 100$ experiments which calculated in finding (RMSE).

We can see in this Figure all the densities of the errors of the parameters seems have shape close to the shape of normal distribution around zero. In another word, the parameters have the consistency and asymptotic normality with mean 0 and exist variance.

6. REAL DATA EXAMPLE

In this sections, we analyzed real data and fitting it to some models considered in this study by composite likelihood and LS-madogram procedures.

6.1. Data analyze. We analyzed daily rainfall on along of east coast of Australia. We selected 39 locations randomly from such region and the daily measured as the total of 24-hours begin from 9 am in the period (April-September) for 35 years from 1982-2016. The data available at Australian Bureau of Meteorology (<http://www.bom.gov.au/climate/data/>).

To explore the possibility of anisotropy of the spatial dependence, we used the same test in [5]. We divided all data set according to directional sectors $(-\pi/8, \pi/8]$, $(\pi/8, 3\pi/8]$, $(3\pi/8, 5\pi/8]$ and $(5\pi/8, 7\pi/8]$, where 0 indicate to north direction. The dependence measures which used in the test

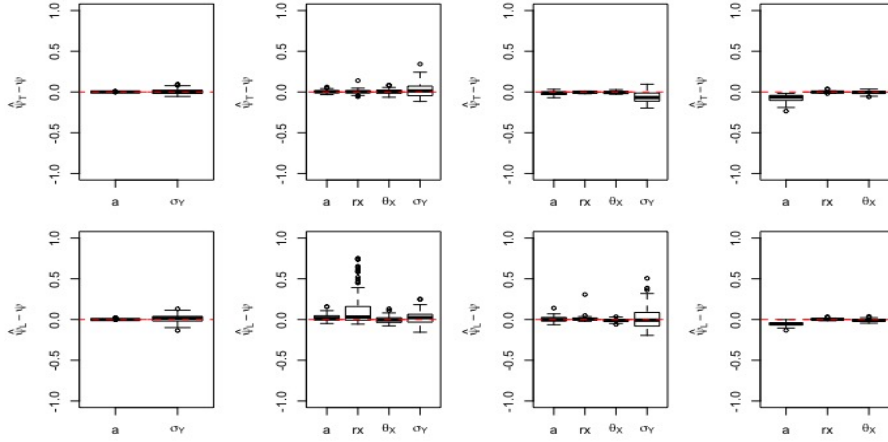


FIGURE 2. Boxplots display $(\hat{\psi} - \psi)$ of estimated parameters vector $\hat{\psi} = (\hat{a}, \hat{r}_X, \hat{\theta}_X, \hat{\sigma}_Y)^T$ for the MM1 model by the two estimators $\hat{\psi}_T$ and $\hat{\psi}_L$. The figures in the first row and from left to right concern the estimator $\hat{\psi}_T$ for $a \in \{0, 0.2, 0.75, 1\}$, the second row concerns $\hat{\psi}_L$. We have set, $r_X = 0.25$, $\theta_X = 0.20$ and $\sigma_Y = 0.6$ over a square $\mathcal{A} = [0, 1]^2$.

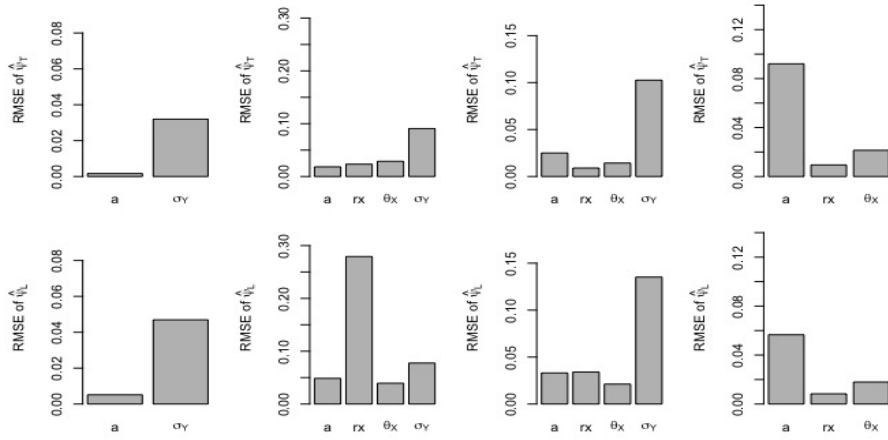


FIGURE 3. Barplots display the RMSE of $\hat{\psi}$ for each estimated parameters $\hat{\psi} = (\hat{a}, \hat{r}_X, \hat{\theta}_X, \hat{\sigma}_Y)^T$ for MM1 and the corresponding two estimators $\hat{\psi}_T$ and $\hat{\psi}_L$. The bars in the first row and from left to right represent the RMSE of the estimator $\hat{\psi}_T$ when $a := \{0, 0.2, 0.75, 1\}$, respectively and the same for the second row for $\hat{\psi}_L$. We set $r_X = 0.25$, $\theta_X = 0.20$ and $\sigma_Y = 0.6$ over a square $\mathcal{A} = [0, 1]^2$.

is the empirical F-madogram $\hat{\nu}^F(h)$. The directional loss smoothing of such empirical measure in the Figure 5. (A), shows that no evidence of anisotropy.

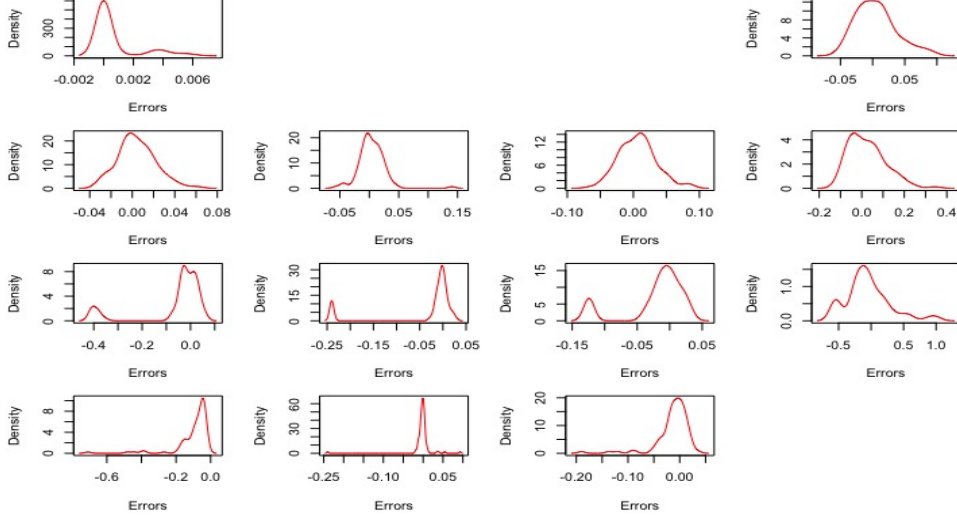


FIGURE 4. Graphs display the densities of the errors between $\hat{\psi}_T$ and ψ_0 for each estimated parameters in the set $\psi = (a, r_X, \theta_X, \sigma_Y)^T$ of MM1 model. These parameters represented by the graphs from the first column to last one respectively. The graphs from first row and last one represent the densities of the estimator $\hat{\psi}_T$ when $a := \{0, 0.2, 0.75, 1\}$, respectively. We set $r_X = 0.25$, $\theta_X = 0.20$ and $\sigma_Y = 0.6$ over a square $\mathcal{A} = [0, 1]^2$.

To comprehension of general behaviour (with respect to dependence structure) of the data set, we evaluated $\hat{\nu}^F(h)$ for all estimated data set. It seems from the loss smoothing behavior in Figure 5. (B) of such evaluation that the asymptotic dependence between the locations to be present up to distance 500 km and asymptotic independence could be present in the remaining distance.

6.2. Data fitting. Our interest in this section is to chose reasonable model can present the data. We considered 7 models described below, for each model, the the parameters estimated by LS-madograme and composite likelihood. The selection criteria for LS-madogram estimator $\hat{\psi}_T$ computed as the following:

$$AIC := \log \mathcal{L}(\hat{\psi}) + (2k(k+1)/(N-k-1)),$$

where k is the number of parameters in a model and N is the number of the observations. Such that, $N = T \times \mathcal{H}$, \mathcal{H} is the number of a pairwise between the sites. With respect to censored composite likelihood estimators we adopted the CLIC selection criteria. The two criteria selected the model MM1 as the best model represent the data.

The models:

MM1: max-mixture between asymptotic dependence process represented by TEG max-stable process X with exponential correlation

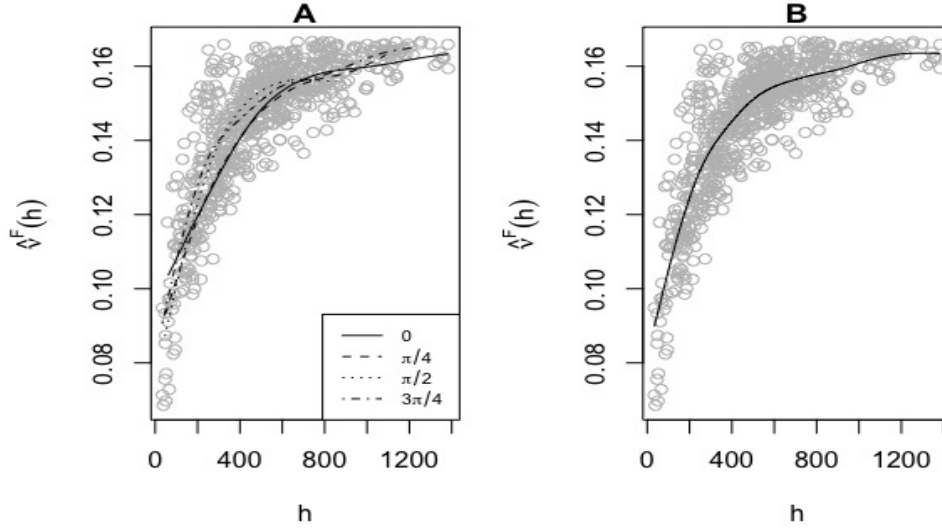


FIGURE 5. Empirical evaluation of $\hat{\nu}^F(h)$. The Grey circles represented the empirical value of between all pairwise. The lines in (A) represent the smoothed value of the empirical of $\hat{\nu}^F(h)$ according to directional sectors $(-\pi/8, \pi/8]$, $(\pi/8, 3\pi/8]$, $(3\pi/8, 5\pi/8]$ and $(5\pi/8, 7\pi/8]$. The line in (B) represent the smoothed value of the empirical of $\hat{\nu}^F(h)$ for all directions.

function $\rho(h) = \exp\{-(h/\theta_X)\}$, $\theta_x > 0$ and \mathcal{B}_X is a disk of fixed and unknown radius r_X and asymptotic independence represented inverse Brown-Resnik max-stable process Y with variogram $2\gamma(h) = 2\sigma^2(1 - \exp\{-(h/\theta_Y)\})$, $\theta_Y, \sigma > 0$. When σ^2 is the sill of the variogram.

MM2: max-mixture between X in MM1 and inverse inverse Smith max-stable process Y with $\tau(h) = h/\sqrt{\sigma_Y}$.

M1: A TEG max-stable process X specified in MM1.

M2: A Brown-Resni max-stable process X specified in MM1.

M3: A inverse Brown-Resnik max-stable process Y specified in MM1.

M4: A Smith max-stable process X specified in M2.

M5: A inverse Smith max-stable process Y specified in M2.

For all models considered, the margin distribution assumed to be unit Fréchet. Therefore require transform the data set to Fréchet. Most of papers for example [5] and [36] used parametric transformation, they fitted GEV parameters for each location separately and then transform the data to Fréchet. In this study, we adopted non-parametric transformation by estimate the margins empirically. For censored composite likelihood procedures, we set $u = 0.9$ and $\delta = \infty$. With respect to AIC and CLIC, we assumed that the data is α -mixing.

TABLE 1. Summary of the fitted models. the distance scale is kilometres. Composite likelihood procedure indicated by CL and LS-madogram procedure indicated by LS with selection criteria SC are CLIC and AIC, respectively.

Model		a	θ_X	r_X	θ_Y	σ_Y	SC
MM1	CL	0.262	1217.3	1364.5	3102.4	3.457	6807406
	LS	0.259	1285.7	1390.0	5794.8	2.013	1.917034
MM2	CL	0.248	31.16	70.15	998.84		7924609
	LS	0.185	35.51	48.14	871.19		1.917234
			θ_X	r_X			CLIC
M1	CL		931	307.86			7926261
	LS		1270	255.64			1.945177
			θ_X	σ_X	θ_Y	σ_Y	CLIC
M2	CL	931.02	3.078663				7926261
	LS	361.36	1.90816				1.96165
M3	CL			1644.76	2.702282		7918643
	LS			1383.08	1.394928		1.924574
M4	CL		85.34				8016633
	LS		193.43				1.988753
M5	CL					256.39	7988838
	LS					334.60	1.929235

7. CONCLUSIONS

We have provided F-madogram $\nu^F(h)$ for the max-mixture process that can detect more than one dependence structure in a model (i.e. asymptotic dependence and asymptotic independence). The F-madogram presents the advantage of having both extremal coefficient $\Theta(h)$ of the max-stable process and $\eta(h)$ of the inverse max-stable in its expression. When $a = 1$, $\nu^F(h)$ is the F-madogram corresponding to a max-stable process introduced by [12] and so switches to $\Theta(h)$; when $a = 0$, $\nu^F(h)$ represents the F-madogram of an inverse max-stable and switches to $\eta(h)$. We defined a semi-parametric estimation procedure using F-madogram $\nu^F(h)$ as an alternative to composite likelihood. The simulation study showed that the estimation procedure based on $\nu^F(h)$ performs better than the composite likelihood procedure when the model is near to asymptotic independence. We applied these estimator procedures to real data example.

REFERENCES

- [1] A. AghaKouchak and N. Nasrollahi, *Semi-parametric and parametric inference of extreme value models for rainfall data*, Water resources management **24** (2010), no. 6, 1229–1249.
- [2] A. Antoniadis, J. Berruyer, and C. René, *Régression non linéaire et applications*, Economica, 1992.
- [3] J-N. Bacro, L. Bel, and C. Lantuéjoul, *Testing the independence of maxima: from bivariate vectors to spatial extreme fields*, Extremes **13** (2010), no. 2, 155–175.
- [4] J-N. Bacro and C. Gaetan, *Estimation of spatial max-stable models using threshold exceedances*, Statistics and Computing **24** (2014), no. 4, 651–662.

- [5] J-N. Bacro, C. Gaetan, and G. Toulemonde, *A flexible dependence model for spatial extremes*, Journal of Statistical Planning and Inference **172** (2016), 36–52.
- [6] J-N. Bacro and G. Toulemonde, *Measuring and modelling multivariate and spatial dependence of extremes*, Journal de la Société Française de Statistique **154** (2013), no. 2, 139–155.
- [7] J. Beirlant, Y. Goegebeur, J. Segers, and J. Teugels, *Statistics of extremes: theory and applications*, John Wiley & Sons, 2006.
- [8] S. Buhl, R. A. Davis, C. Klüppelberg, and C. Steinkohl, *Semiparametric estimation for isotropic max-stable space-time processes*, submitted (2016).
- [9] T.A. Buishand, *Bivariate extreme-value data and the station-year method*, Journal of Hydrology **69** (1984), no. 1, 77–95.
- [10] S. Coles, J. Bawa, L. Trenner, and P. Dorazio, *An introduction to statistical modeling of extreme values*, Vol. 208, Springer, 2001.
- [11] S. Coles, J. Heffernan, and J.A. Tawn, *Dependence measures for extreme value analyses*, Extremes **2** (1999), no. 4, 339–365.
- [12] D. Cooley, P. Naveau, and P. Poncet, *Variograms for spatial max-stable random fields*, Dependence in probability and statistics, 2006, pp. 373–390.
- [13] R. A. Davis and C. Y. Yau, *Comments on pairwise likelihood in time series models*, Statistica Sinica (2011), 255–277.
- [14] A. C. Davison and M. Gholamrezaee, *Geostatistics of extremes*, Proceedings of the royal society of london a: Mathematical, physical and engineering sciences, 2012, pp. 581–608.
- [15] A.C. Davison, R. Huser, and E. Thibaud, *Geostatistics of dependent and asymptotically independent extremes*, Mathematical Geosciences **45** (2013), no. 5, 511–529.
- [16] L. De Haan, *A spectral representation for max-stable processes*, The annals of probability (1984), 1194–1204.
- [17] L. De Haan and T. T. Pereira, *Spatial extremes: Models for the stationary case*, The annals of statistics (2006), 146–168.
- [18] C. Edward, *The use of subseries values for estimating the variance of a general statistic from a stationary sequence*, The Annals of Statistics (1986), 1171–1179.
- [19] C. Fonseca, L. Pereira, H. Ferreira, and A.P. Martins, *Generalized madogram and pairwise dependence of maxima over two regions of a random field*, KYBERNETIKE **51** (2015), no. 2, 193–211.
- [20] A. Guillou, P. Naveau, and A. Schorgen, *Madogram and asymptotic independence among maxima*, REVSTAT—Statistical Journal **12** (2014), no. 2, 119–134.
- [21] X. Guyon, *Random fields on a network: modeling, statistics, and applications*, Springer Science & Business Media, 1995.
- [22] Z. Kabluchko, M. Schlather, and L. De Haan, *Stationary max-stable fields associated to negative definite functions*, The Annals of Probability (2009), 2042–2065.
- [23] A.W. Ledford and J.A. Tawn, *Statistics for near independence in multivariate extreme values*, Biometrika **83** (1996), no. 1, 169–187.
- [24] B.G. Lindsay, *Composite likelihood methods*, Contemporary Math. (1988), 221–239.
- [25] P. Naveau, A. Guillou, D. Cooley, and J. Diebolt, *Modelling pairwise dependence of maxima in space*, Biometrika **96** (2009), no. 1, 1–17.
- [26] P. J. Northrop, *An efficient semiparametric maxima estimator of the extremal index*, Extremes **18** (2015), no. 4, 585–603.
- [27] S. A. Padoan, M. Ribatet, and S. A. Sisson, *Likelihood-based inference for max-stable processes*, Journal of the American Statistical Association **105** (2010), no. 489, 263–277.
- [28] M. Schlather, *Models for stationary max-stable random fields*, Extremes **5** (2002), no. 1, 33–44.
- [29] M. Schlather and J.A. Tawn, *A dependence measure for multivariate and spatial extreme values: Properties and inference*, Biometrika **90** (2003), no. 1, 139–156.
- [30] M. Sibuya, *Bivariate extreme statistics, i*, Annals of the Institute of Statistical Mathematics **11** (1959), no. 2, 195–210.
- [31] R. L. Smith, *Max-stable processes and spatial extremes*, Unpublished manuscript, Univer (1990).

- [32] E. Thibaud, R. Mutzner, and A.C. Davison, *Threshold modeling of extreme spatial rainfall*, *Water resources research* **49** (2013), no. 8, 4633–4644.
- [33] C. Varin, N. Reid, and D. Firth, *An overview of composite likelihood methods*, *Statistica Sinica* (2011), 5–42.
- [34] C. Varin and P. Vidoni, *A note on composite likelihood inference and model selection*, *Biometrika* (2005), 519–528.
- [35] H. Wackernagel, *Multivariate nested variogram*, *Multivariate geostatistics*, 1998, pp. 172–180.
- [36] J.L. Wadsworth and J.A. Tawn, *Dependence modelling for spatial extremes*, *Biometrika* **99** (2012), no. 2, 253–272.
- [37] F. Zheng, E. Thibaud, M. Leonard, and S. Westra, *Assessing the performance of the independence method in modeling spatial extreme rainfall*, *Water Resources Research* **51** (2015), no. 9, 7744–7758.
- [38] F. Zheng, S. Westra, M. Leonard, and S. A. Sisson, *Modeling dependence between extreme rainfall and storm surge to estimate coastal flooding risk*, *Water Resources Research* **50** (2014), no. 3, 2050–2071.

UNIVERSITÉ DE LYON, UNIVERSITÉ LYON 1, INSTITUT CAMILLE JORDAN ICJ UMR
5208 CNRS, FRANCE, DEPARTMENT OF STATISTICS, UNIVERSITY OF MOSUL, IRAQ

UNIVERSITÉ DE LYON, UNIVERSITÉ LYON 1, INSTITUT CAMILLE JORDAN ICJ UMR
5208 CNRS, FRANCE

UNIVERSITÉ DE LYON, UNIVERSITÉ LYON 1, INSTITUT CAMILLE JORDAN ICJ UMR
5208 CNRS, FRANCE

UNIVERSITÉ DE LYON, UNIVERSITÉ LYON 1, INSTITUT CAMILLE JORDAN ICJ UMR
5208 CNRS, FRANCE